

NLO electroweak and QCD corrections to off-shell $t\bar{t}W$ production at the LHC

A. Denner¹ and G. Pelliccioli^{1*}

¹ University of Würzburg, Institut für Theoretische Physik und Astrophysik, Emil-Hilb-Weg 22, 97074 Würzburg (Germany)

* giovanni.pelliccioli@physik.uni-wuerzburg.de

November 15, 2022



*15th International Symposium on Radiative Corrections:
Applications of Quantum Field Theory to Phenomenology,
FSU, Tallahassee, FL, USA, 17-21 May 2021*
doi:[10.21468/SciPostPhysProc.7](https://doi.org/10.21468/SciPostPhysProc.7)

Abstract

The foreseen luminosities for the next LHC runs will enable precise differential measurements of the associated production of top–antitop pairs with a W boson. Therefore, providing accurate theory predictions for this process is needed for realistic final states. We present the first combination of NLO electroweak and QCD corrections to off-shell $t\bar{t}W^+$ production in the three-charged-lepton channel, including non-resonant effects, full spin-correlations and interferences. Such radiative corrections comprise the electroweak and QCD corrections to the leading QCD order, and the QCD corrections to the leading electroweak order.

1 Introduction

The associated production of top–antitop pairs with W bosons represents one of the heaviest signatures at the LHC and an important process to study, both as a probe of the Standard Model (SM) and as a window to new-physics effects. It gives direct access to the coupling of top quarks to electroweak (EW) bosons in or beyond the SM [1–3] and it is expected to enhance the sensitivity to the $t\bar{t}$ charge asymmetry [4]. This process is also a relevant background to the associated $t\bar{t}$ production with a Higgs boson [5]. Recent ATLAS and CMS public results [6, 7] and improved analyses [8, 9] for $t\bar{t}W$ point in the direction of a tension between data and SM predictions, which has not been addressed yet in spite of strong efforts in the theoretical community. Since the high-luminosity run of the LHC will allow for differential measurements in $t\bar{t}W$, it is essential to provide precise SM predictions for this process in specific decay channels. The next-to-leading-order (NLO) QCD and EW corrections are known since several years for the inclusive production [4, 5, 10–12]. Soft-gluon resummation [13–17] and multi-jet merging [18, 19] have been performed for inclusive production. The decay modelling has been tackled in the narrow-width approximation (NWA) at NLO QCD [20] and with matching to parton shower [21]. The subleading NLO QCD corrections to the LO EW have been computed in the NWA, including spin correlations and parton-shower effects [22, 23]. The first predictions for off-shell $t\bar{t}W$ production in the three-charged-lepton

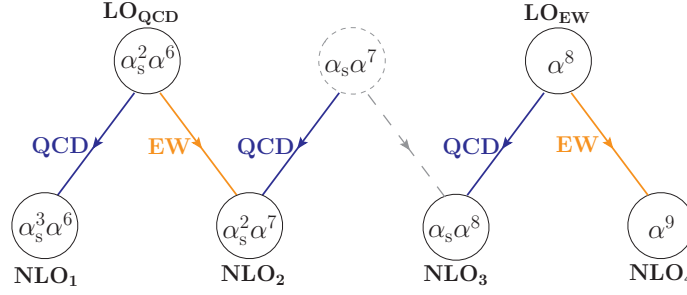


Figure 1: Perturbative orders contributing at LO and NLO to $t\bar{t}W$ production in the three-charged-lepton decay channel.

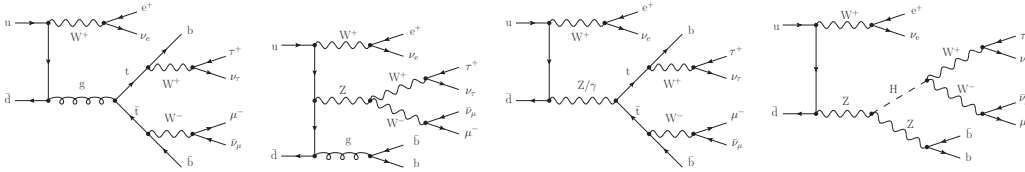


Figure 2: Sample diagrams contributing to LO_{QCD} (left) and to LO_{EW} (right) cross-sections for off-shell $t\bar{t}W^+$ production in the three-charged-lepton decay channel.

channel have appeared recently [24–26] and have been also compared to NWA results matched with parton-shower [27]. Based on Ref. [28], we present the first complete fixed-order description of the off-shell production of $t\bar{t}W^+$ in the three-charged-lepton decay channel, combining NLO QCD and EW corrections which are sizeable at the LHC@13TeV.

2 Description of the calculation

We consider the process $pp \rightarrow e^+ \nu_e \tau^+ \nu_\tau \mu^- \bar{\nu}_\mu b \bar{b} + X$. At LO exclusively quark-induced partonic channels contribute, while at NLO the gluon–quark and photon–quark channels open up. The gluon–gluon channel only enters the calculation at NNLO QCD. This process, embedding as dominant resonant structure a $t\bar{t}$ pair in association with a W^+ boson, receives contributions from three different coupling orders at LO, as can be observed in Fig. 1: the largest contribution (labelled LO_{QCD}) is of order $\mathcal{O}(\alpha_s^2 \alpha^6)$, while the $\mathcal{O}(\alpha^8)$ contribution (labelled LO_{EW}) is roughly 1% of LO_{QCD} . Sample diagrams are shown in Fig. 2. The interference among QCD and EW diagrams, of order $\mathcal{O}(\alpha_s \alpha^7)$, vanishes owing to colour algebra (in the case of a diagonal CKM matrix with unit entries). Both at LO_{QCD} and at LO_{EW} , diagrams with two, one, or zero resonant top/antitop quarks are present in the off-shell calculation.

At NLO, four coupling orders contribute to $t\bar{t}W$ hadro-production (see Fig. 1). The pure QCD corrections to LO_{QCD} (labelled NLO_1), of order $\mathcal{O}(\alpha_s^3 \alpha^6)$, are the dominant ones at NLO. The corresponding virtual corrections involve up to 7-point functions, while the real corrections are challenging due to the high multiplicity of particle in the final state. The NLO_1 corrections to off-shell $t\bar{t}W$, calculated by two independent groups [24, 25], are strongly dependent on the (renormalization and factorization) central-scale choice and range between 10% and 20% of the LO_{QCD} cross-section.

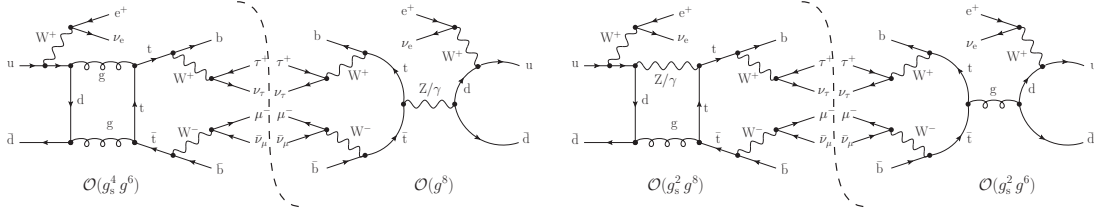


Figure 3: Sample $\mathcal{O}(\alpha_s^2 \alpha^7)$ virtual corrections to off-shell $t\bar{t}W$ production in the three-charged-lepton decay channel: QCD corrections to the LO interference (left) and mixed contribution (right).

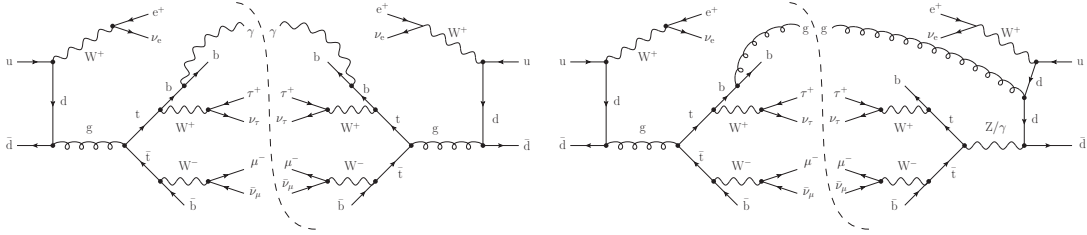


Figure 4: Sample $\mathcal{O}(\alpha_s^2 \alpha^7)$ real corrections to off-shell $t\bar{t}W$ production in the three-charged-lepton decay channel: EW corrections to LO_{QCD} (left) and QCD corrections to the LO interference (right).

The corrections of order $\mathcal{O}(\alpha_s^2 \alpha^7)$, labelled NLO_2 , come from the EW radiative corrections to LO_{QCD} as well as from the QCD corrections to the LO interference, even though the contribution of order $\mathcal{O}(\alpha_s \alpha^7)$ vanishes. The corresponding virtual corrections require up to 10-point functions to be evaluated, and can be divided in two classes (see Fig. 3): one-loop amplitudes of order $\mathcal{O}(g_s^4 g^6)$ contracted with tree-level amplitudes of order $\mathcal{O}(g^8)$ and one-loop amplitudes of order $\mathcal{O}(g_s^2 g^8)$ contracted with tree-level amplitudes of order $\mathcal{O}(g_s^2 g^6)$. Analogously, the real corrections receive contributions from photon radiation off LO_{QCD} squared amplitudes as well as from gluon radiation off the LO interference. Sample diagrams for real radiation at this perturbative order are shown in Fig. 4. It is crucial to include both EW corrections to LO_{QCD} and QCD corrections to the LO interference to ensure the infrared (IR) finiteness of the NLO correction. In fact, the IR singularities in one-loop amplitudes of order $\mathcal{O}(g_s^2 g^8)$ (right side of Fig. 3) are cancelled by both classes of real-radiation contributions (Fig. 4).

Since the LO interference vanishes, the corresponding EW corrections vanish as well. Therefore, the NLO_3 corrections, of order $\mathcal{O}(\alpha_s \alpha^8)$, are pure QCD corrections to LO_{EW} . Such corrections, although expected to be sub-leading w.r.t. the NLO_1 and NLO_2 ones by α_s -power counting arguments, give a larger contribution than the NLO_2 ones at the inclusive level [10, 12], as they are dominated by real radiation contributions in the quark–gluon partonic channel which embed the tW^+ scattering as a sub-process [1].

The pure EW corrections to LO_{EW} , formally of order $\mathcal{O}(\alpha^9)$, have been shown to be at the sub-mille level [11, 12] and will be hardly relevant even at the high-luminosity LHC. Therefore they are not considered in this context.

One-loop and tree-level amplitudes are calculated with RECOLA [29, 30], interfaced with COLLIER [31] for the reduction and evaluation of loop integrals. The Monte Carlo integration is performed via a multi-channel approach with the MOCANLO code, which has already been utilized

order	$\mu_0^{(c)}$		$\mu_0^{(d)}$		$\mu_0^{(e)}$	
	σ (fb)	ratio	σ (fb)	ratio	σ (fb)	ratio
LO _{QCD} ($\alpha_s^2 \alpha^6$)	0.2218(1) ^{+25.3%} _{-18.8%}	1	0.1948(1) ^{+23.9%} _{-18.1%}	1	0.2414(1) ^{+26.2%} _{-19.3%}	1
LO _{EW} (α^8)	0.002164(1) ^{+3.7%} _{-3.6%}	0.010	0.002122(1) ^{+3.7%} _{-3.6%}	0.011	0.002201(1) ^{+3.7%} _{-3.6%}	0.009
NLO ₁ ($\alpha_s^3 \alpha^6$)	0.0147(6)	0.066	0.0349(6)	0.179	0.0009(7)	0.004
NLO ₂ ($\alpha_s^2 \alpha^7$)	-0.0122(3)	-0.055	-0.0106(3)	-0.054	-0.0134(4)	-0.056
NLO ₃ ($\alpha_s \alpha^8$)	0.0293(1)	0.131	0.0263(1)	0.135	0.0320(1)	0.133
LO _{QCD} +NLO ₁	0.2365(6) ^{+2.9%} _{-6.0%}	1.066	0.2297(6) ^{+5.5%} _{-7.3%}	1.179	0.2423(7) ^{+3.5%} _{-5.2%}	1.004
LO _{QCD} +NLO ₂	0.2094(3) ^{+25.0%} _{-18.7%}	0.945	0.1840(3) ^{+23.8%} _{-17.9%}	0.946	0.2277(4) ^{+25.9%} _{-19.2%}	0.944
LO _{EW} +NLO ₃	0.03142(4) ^{+22.2%} _{-16.8%}	0.141	0.02843(6) ^{+20.5%} _{-15.6%}	0.146	0.03425(7) ^{+22.8%} _{-17.0%}	0.142
LO+NLO	0.2554(7) ^{+4.0%} _{-6.5%}	1.151	0.2473(7) ^{+6.3%} _{-7.6%}	1.270	0.2628(9) ^{+4.3%} _{-5.9%}	1.089

Table 1: Fiducial LO cross-sections and NLO corrections (in fb) for three different central-scale choices [see Eq. (1)]. Scale uncertainties from 7-point scale variations are shown in percentages. Ratios are relative to the LO_{QCD} cross-sections.

for several LHC processes with top quarks [32, 33] and now for $t\bar{t}W$ [25, 28]. The subtraction of IR singularities is performed in the dipole scheme [34–36]. Top-quark and EW-boson masses, as well as the weak mixing angle are treated in the complex-mass scheme [37–41]. Full off-shell matrix elements are considered at LO and NLO, including finite-width and non-resonant effects, as well as complete spin correlations. For more information on input parameters and details of the calculation, we refer to Sect. (2.2) of Ref. [28].

3 Phenomenological results

We now present phenomenological results for a fiducial LHC setup that mimics the signal region defined in a recent ATLAS measurement [7]. For more details on the selection cuts we refer to Sect. (2.3) of Ref. [28]. In Table 1 we show integrated results for LO cross-sections and NLO corrections, for three different choices of renormalization and factorization scale (labelled following the notation of Ref. [25]),

$$\mu_0^{(c)} = \frac{1}{3} \left(p_{T,\text{miss}} + \sum_{i=b,\ell} p_{T,i} \right), \quad \mu_0^{(d)} = \sqrt{\sqrt{m_t^2 + p_{T,t}^2} \sqrt{m_t^2 + p_{T,\bar{t}}^2}}, \quad \mu_0^{(e)} = \frac{\mu_0^{(d)}}{2}, \quad (1)$$

where the ambiguity in identifying the top quark (for scale choices $\mu_0^{(d)}$ and $\mu_0^{(e)}$) is resolved by selecting decay products that give an invariant mass closer to the top-quark pole mass.

The impact of NLO₁ corrections relative to the LO_{QCD} cross-section is scale dependent, and such corrections range between +0.5% and +18% depending on the central-scale choice. At variance with NLO₁, the relative NLO₂ and NLO₃ corrections are rather scale independent and amount to -5% and +13% of the LO_{QCD} result, respectively. As expected from power counting, the LO_{EW} cross-section is about 1% of the LO_{QCD} one, while the NLO₃ corrections are 10-times larger than LO_{EW}, giving more sizeable corrections than the NLO₂ ones, in spite of one power of α_s less. Also in the off-shell calculation, hard real corrections embedding the tW scattering dominate the $\mathcal{O}(\alpha_s^3 \alpha^6)$ perturbative order, confirming the inclusive results [10, 12]. The NLO

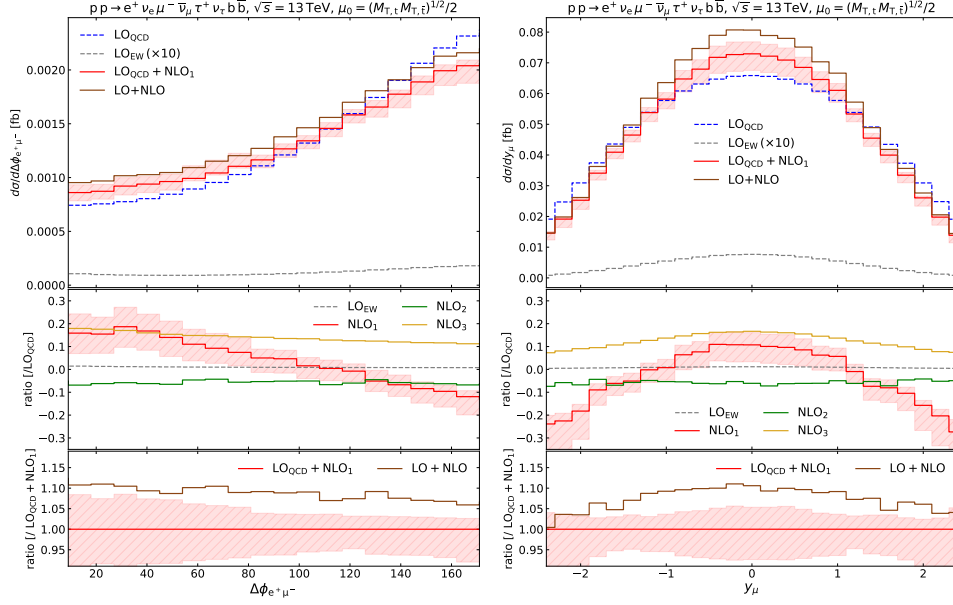


Figure 5: Distributions in the azimuthal separation between the positron and the muon (left) and in the muon rapidity (right). Top: differential cross-sections in fb for LO_{QCD} , LO_{EW} , $\text{LO}_{\text{QCD}} + \text{NLO}_1$ and for complete NLO (sum of all LO cross-sections and NLO corrections). Middle: ratios of LO_{EW} , NLO_1 , NLO_2 , and NLO_3 corrections over the LO_{QCD} cross-section. Bottom: ratios of LO+NLO cross-section over the $\text{LO}_{\text{QCD}} + \text{NLO}_1$ one. Uncertainties from seven-point scale variations are shown for $\text{LO}_{\text{QCD}} + \text{NLO}_1$ distributions.

corrections, obtained combining NLO_1 , NLO_2 , and NLO_3 in an additive way, range between +9% and +27%, depending on the central-scale choice. The scale uncertainties at NLO are at the 5% level and are dominated by NLO_1 corrections. The NLO_2 corrections have been calculated also in a very inclusive setup, obtaining similar relative corrections to the LO_{QCD} cross-section (−3%) as in on-shell calculations [12].

In Figs. 5–7 we present differential results for the scale choice $\mu_0^{(e)}$. For exclusive observables, the interplay among the three NLO corrections can differ sizeably from the results obtained for total cross-sections.

In the left panel of Fig. 5 we show the distributions in the azimuthal separation between the positron and the muon. The NLO corrections increase the rate of events with small azimuthal separation. The NLO_1 corrections diminish from +18% to +11% with constant slope over the distribution range, while the NLO_2 and NLO_3 ones give a rather constant shift to the $\text{LO}_{\text{QCD}} + \text{NLO}_1$ cross-section.

In the right panel of Fig. 5 we consider distributions in the muon rapidity. This observable represents a good proxy for the rapidity of the antitop quark [28]. The muon is preferably produced with central rapidity. The NLO_2 corrections give an almost flat negative shift to the LO_{QCD} differential cross-section, while the relative NLO_1 corrections feature a variation of about 35% in the rapidity range. The shape of NLO_3 corrections (relatively to LO_{QCD}) is similar to the one of NLO_1 corrections. Such corrections give a positive shift to the LO cross-section, ranging from +16% (central region) to +8% (forward regions).

In the left panel of Fig. 6 the distributions in the antitop-quark invariant mass are shown. The

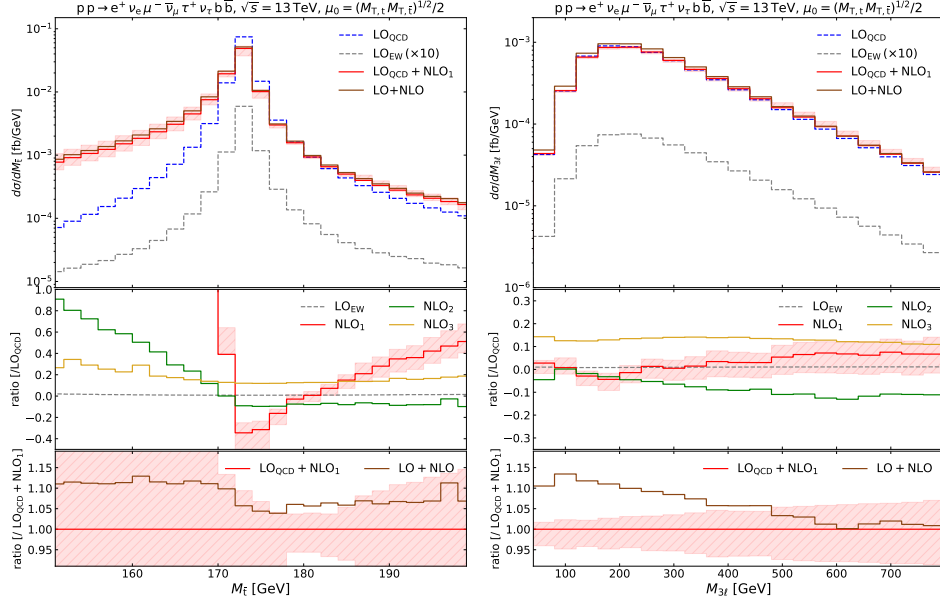


Figure 6: Distributions in the invariant mass of the antitop quark (left) and of the three-charged-lepton system (right). Same structure as Fig. 5.

antitop-quark system ($\bar{b}\mu^-\bar{\nu}_\mu$) is only known from the Monte Carlo truth, owing to the presence of three neutrinos in the final state. The NLO_1 corrections are negative near the Breit–Wigner peak, while they give a huge radiative enhancement to LO_{QCD} below the top-quark pole mass, coming from real gluon radiation that is not clustered into b jets. A similar radiative tail, though less sizeable, is found also for NLO_2 corrections. For an invariant mass larger than the pole mass, NLO_1 relative corrections increase towards positive values while the NLO_2 ones give an almost flat negative shift to LO_{QCD} (-10%). At variance with NLO_1 and NLO_2 , the NLO_3 corrections are rather flat, ranging between $+10\%$ at the peak and $+30\%$ in the tail region, due to the large quark–gluon partonic channel, which features a light quark as final-state particle, which cannot result from the radiative decay of top/antitop quarks.

In the right panel of Fig. 6 we consider the invariant mass of the system formed by the three charged leptons. The QCD corrections (NLO_1 and NLO_3) are rather flat, while the NLO_2 corrections, dominated by virtual EW corrections, negatively increase towards large masses (-10% around 500 GeV). Such a behaviour is driven by Sudakov logarithms, which become large at high energy.

An analogous effect is found for transverse-momentum distributions, that are considered in Fig. 7. In fact, large negative NLO_2 corrections are found in the tail of the transverse-momentum distribution for the reconstructed antitop quark (-20% at 800 GeV) as well as for the two-b-jet system (-20% at 350 GeV). The NLO_3 corrections are pretty flat for both observables considered in Fig. 7, ranging between $+10\%$ and $+30\%$ in the considered transverse-momentum ranges. The NLO_1 corrections increase by 25% from small to large p_T of the antitop quark, while they become much larger at moderate values of the transverse momentum of the two-b-jet system. The two-b-jet system is correlated to the $t\bar{t}$ system [25], which recoils against a W^+ boson and thus receives large contributions from unclustered real QCD radiation. The combined NLO corrections to the $b\bar{b}$ -system transverse momentum is almost vanishing due to cancellation among different

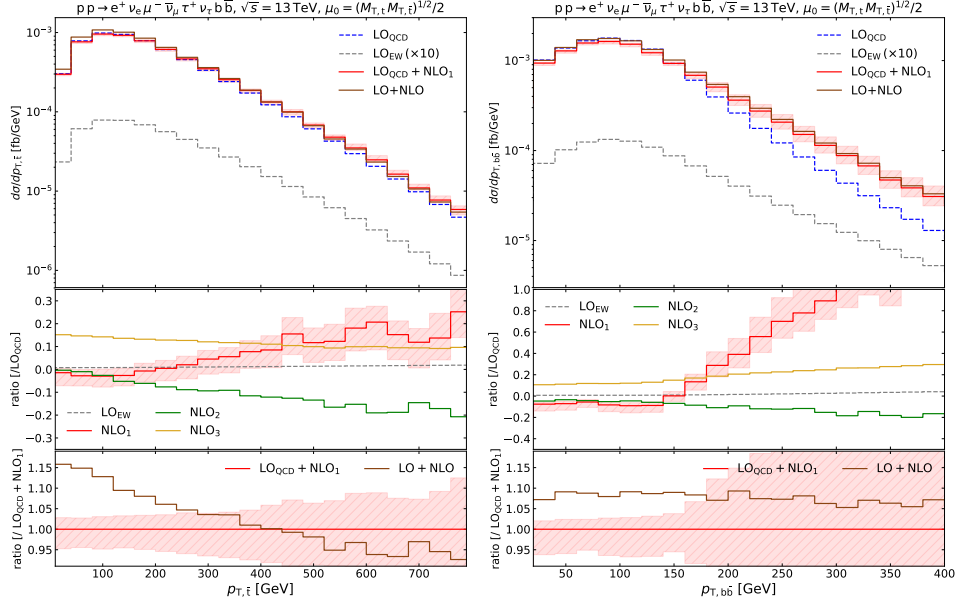


Figure 7: Distributions in the transverse momentum of the antitop quark (left) and of the two-b-jet system (right). Same structure as Fig. 5.

contributions in the soft region of the spectrum, while it is dominated by NLO_1 corrections for $p_{T,b\bar{b}} > 150$ GeV.

Both angular (Fig. 5) and energy-dependent distributions (Figs. 6–7) show that the combined NLO predictions exceed the scale uncertainties of the NLO QCD results ($LO_{QCD} + NLO_1$) also in most populated kinematic regions, *e.g.* soft transverse momentum and central rapidity.

4 Conclusion

We have presented the first calculation including complete off-shell effects at NLO QCD [$\mathcal{O}(\alpha_s^3 \alpha^6)$] and subleading NLO orders [$\mathcal{O}(\alpha_s^2 \alpha^7)$ and $\mathcal{O}(\alpha_s \alpha^8)$] for the hadronic production of $t\bar{t}W^+$ in the three-charged-lepton decay channel. The NLO_1 corrections range between +0.5% and +18%, depending on the central-scale choice. The scale uncertainties are reduced from 25% to 5% from LO to NLO, driven by the NLO_1 corrections. The NLO_2 corrections are negative (about -5%) and independent of the scale choice (relative to the LO cross-section), but they become large (up to -20%) for high-energy regimes in transverse-momentum and invariant-mass distributions. The NLO_3 corrections are also large, ranging between +10% and +30% in the considered distributions, and are rather scale independent. These corrections are dominated by gluon–quark-induced contributions embedding the tW -scattering process. The inclusion of NLO_2 and NLO_3 corrections is necessary for the modelling of $t\bar{t}W^+$ production, as all NLO contributions change sizeably distribution shapes. Furthermore, the off-shell effects become important in the tails of several distributions.

Acknowledgements

This work is supported by the German Federal Ministry for Education and Research (BMBF) under contract no. 05H18WWCA1.

References

- [1] J. A. Dror, M. Farina, E. Salvioni and J. Serra, *Strong tW Scattering at the LHC*, JHEP **01**, 071 (2016), doi:[10.1007/JHEP01\(2016\)071](https://doi.org/10.1007/JHEP01(2016)071), [1511.03674](https://arxiv.org/abs/1511.03674).
- [2] A. Buckley, C. Englert, J. Ferrando, D. J. Miller, L. Moore, M. Russell and C. D. White, *Constraining top quark effective theory in the LHC Run II era*, JHEP **04**, 015 (2016), doi:[10.1007/JHEP04\(2016\)015](https://doi.org/10.1007/JHEP04(2016)015), [1512.03360](https://arxiv.org/abs/1512.03360).
- [3] O. Bessidskaia Bylund, F. Maltoni, I. Tsinikos, E. Vryonidou and C. Zhang, *Probing top quark neutral couplings in the Standard Model Effective Field Theory at NLO in QCD*, JHEP **05**, 052 (2016), doi:[10.1007/JHEP05\(2016\)052](https://doi.org/10.1007/JHEP05(2016)052), [1601.08193](https://arxiv.org/abs/1601.08193).
- [4] F. Maltoni, M. Mangano, I. Tsinikos and M. Zaro, *Top-quark charge asymmetry and polarization in $t\bar{t}W^\pm$ production at the LHC*, Phys. Lett. B **736**, 252 (2014), doi:[10.1016/j.physletb.2014.07.033](https://doi.org/10.1016/j.physletb.2014.07.033), [1406.3262](https://arxiv.org/abs/1406.3262).
- [5] F. Maltoni, D. Pagani and I. Tsinikos, *Associated production of a top-quark pair with vector bosons at NLO in QCD: impact on $t\bar{t}H$ searches at the LHC*, JHEP **02**, 113 (2016), doi:[10.1007/JHEP02\(2016\)113](https://doi.org/10.1007/JHEP02(2016)113), [1507.05640](https://arxiv.org/abs/1507.05640).
- [6] A. M. Sirunyan *et al.*, *Measurement of the cross section for top quark pair production in association with a W or Z boson in proton-proton collisions at $\sqrt{s} = 13$ TeV*, JHEP **08**, 011 (2018), doi:[10.1007/JHEP08\(2018\)011](https://doi.org/10.1007/JHEP08(2018)011), [1711.02547](https://arxiv.org/abs/1711.02547).
- [7] M. Aaboud *et al.*, *Measurement of the $t\bar{t}Z$ and $t\bar{t}W$ cross sections in proton-proton collisions at $\sqrt{s} = 13$ TeV with the ATLAS detector*, Phys. Rev. **D99**, 072009 (2019), doi:[10.1103/PhysRevD.99.072009](https://doi.org/10.1103/PhysRevD.99.072009), [1901.03584](https://arxiv.org/abs/1901.03584).
- [8] *Analysis of $t\bar{t}H$ and $t\bar{t}W$ production in multilepton final states with the ATLAS detector*, Tech. Rep. ATLAS-CONF-2019-045, CERN, Geneva (2019).
- [9] *Search for Higgs boson production in association with top quarks in multilepton final states at $\sqrt{s} = 13$ TeV*, Tech. Rep. CMS-PAS-HIG-17-004, CERN, Geneva (2017).
- [10] S. Frixione, V. Hirschi, D. Pagani, H. S. Shao and M. Zaro, *Electroweak and QCD corrections to top-pair hadroproduction in association with heavy bosons*, JHEP **06**, 184 (2015), doi:[10.1007/JHEP06\(2015\)184](https://doi.org/10.1007/JHEP06(2015)184), [1504.03446](https://arxiv.org/abs/1504.03446).
- [11] R. Frederix, D. Pagani and M. Zaro, *Large NLO corrections in $t\bar{t}W^\pm$ and $t\bar{t}t\bar{t}$ hadroproduction from supposedly subleading EW contributions*, JHEP **02**, 031 (2018), doi:[10.1007/JHEP02\(2018\)031](https://doi.org/10.1007/JHEP02(2018)031), [1711.02116](https://arxiv.org/abs/1711.02116).

- [12] R. Frederix, S. Frixione, V. Hirschi, D. Pagani, H.-S. Shao and M. Zaro, *The automation of next-to-leading order electroweak calculations*, JHEP **07**, 185 (2018), doi:[10.1007/JHEP07\(2018\)185](https://doi.org/10.1007/JHEP07(2018)185), [1804.10017](https://arxiv.org/abs/1804.10017).
- [13] H. T. Li, C. S. Li and S. A. Li, *Renormalization group improved predictions for $t\bar{t}W^\pm$ production at hadron colliders*, Phys. Rev. D **90**, 094009 (2014), doi:[10.1103/PhysRevD.90.094009](https://doi.org/10.1103/PhysRevD.90.094009), [1409.1460](https://arxiv.org/abs/1409.1460).
- [14] A. Broggio, A. Ferroglia, G. Ossola and B. D. Pecjak, *Associated production of a top pair and a W boson at next-to-next-to-leading logarithmic accuracy*, JHEP **09**, 089 (2016), doi:[10.1007/JHEP09\(2016\)089](https://doi.org/10.1007/JHEP09(2016)089), [1607.05303](https://arxiv.org/abs/1607.05303).
- [15] A. Kulesza, L. Motyka, D. Schwartländer, T. Stebel and V. Theeuwes, *Associated production of a top quark pair with a heavy electroweak gauge boson at NLO+NNLL accuracy*, Eur. Phys. J. C **79**, 249 (2019), doi:[10.1140/epjc/s10052-019-6746-z](https://doi.org/10.1140/epjc/s10052-019-6746-z), [1812.08622](https://arxiv.org/abs/1812.08622).
- [16] A. Broggio, A. Ferroglia, R. Frederix, D. Pagani, B. D. Pecjak and I. Tsinikos, *Top-quark pair hadroproduction in association with a heavy boson at NLO+NNLL including EW corrections*, JHEP **08**, 039 (2019), doi:[10.1007/JHEP08\(2019\)039](https://doi.org/10.1007/JHEP08(2019)039), [1907.04343](https://arxiv.org/abs/1907.04343).
- [17] A. Kulesza, L. Motyka, D. Schwartländer, T. Stebel and V. Theeuwes, *Associated top quark pair production with a heavy boson: differential cross sections at NLO+NNLL accuracy*, Eur. Phys. J. C **80**, 428 (2020), doi:[10.1140/epjc/s10052-020-7987-6](https://doi.org/10.1140/epjc/s10052-020-7987-6), [2001.03031](https://arxiv.org/abs/2001.03031).
- [18] S. von Buddenbrock, R. Ruiz and B. Mellado, *Anatomy of inclusive $t\bar{t}W$ production at hadron colliders*, Phys. Lett. B **811**, 135964 (2020), doi:[10.1016/j.physletb.2020.135964](https://doi.org/10.1016/j.physletb.2020.135964), [2009.00032](https://arxiv.org/abs/2009.00032).
- [19] R. Frederix and I. Tsinikos, *On improving NLO merging for $t\bar{t}W$ production* (2021), [2108.07826](https://arxiv.org/abs/2108.07826).
- [20] J. M. Campbell and R. K. Ellis, *$t\bar{t}W^\pm$ production and decay at NLO*, JHEP **07**, 052 (2012), doi:[10.1007/JHEP07\(2012\)052](https://doi.org/10.1007/JHEP07(2012)052), [1204.5678](https://arxiv.org/abs/1204.5678).
- [21] M. V. Garzelli, A. Kardos, C. G. Papadopoulos and Z. Trócsányi, *$t\bar{t}W^\pm$ and $t\bar{t}Z$ Hadroproduction at NLO accuracy in QCD with Parton Shower and Hadronization effects*, JHEP **11**, 056 (2012), doi:[10.1007/JHEP11\(2012\)056](https://doi.org/10.1007/JHEP11(2012)056), [1208.2665](https://arxiv.org/abs/1208.2665).
- [22] R. Frederix and I. Tsinikos, *Subleading EW corrections and spin-correlation effects in $t\bar{t}W$ multi-lepton signatures*, Eur. Phys. J. C **80**, 803 (2020), doi:[10.1140/epjc/s10052-020-8388-6](https://doi.org/10.1140/epjc/s10052-020-8388-6), [2004.09552](https://arxiv.org/abs/2004.09552).
- [23] F. F. Cordero, M. Kraus and L. Reina, *Top-quark pair production in association with a W^\pm gauge boson in the POWHEG-BOX*, Phys. Rev. D **103**(9), 094014 (2021), doi:[10.1103/PhysRevD.103.094014](https://doi.org/10.1103/PhysRevD.103.094014), [2101.11808](https://arxiv.org/abs/2101.11808).
- [24] G. Bevilacqua, H.-Y. Bi, H. B. Hartanto, M. Kraus and M. Worek, *The simplest of them all: $t\bar{t}W^\pm$ at NLO accuracy in QCD*, JHEP **08**, 043 (2020), doi:[10.1007/JHEP08\(2020\)043](https://doi.org/10.1007/JHEP08(2020)043), [2005.09427](https://arxiv.org/abs/2005.09427).
- [25] A. Denner and G. Pelliccioli, *NLO QCD corrections to off-shell $t\bar{t}W^+$ production at the LHC*, JHEP **11**, 069 (2020), doi:[10.1007/JHEP11\(2020\)069](https://doi.org/10.1007/JHEP11(2020)069), [2007.12089](https://arxiv.org/abs/2007.12089).

- [26] G. Bevilacqua, H.-Y. Bi, H. B. Hartanto, M. Kraus, J. Nasufi and M. Worek, *NLO QCD corrections to off-shell $t\bar{t}W^\pm$ production at the LHC: Correlations and Asymmetries*, Eur. Phys. J. C **81**, 675 (2021), doi:[10.1140/epjc/s10052-021-09478-x](https://doi.org/10.1140/epjc/s10052-021-09478-x), [2012.01363](https://arxiv.org/abs/2012.01363).
- [27] G. Bevilacqua, H. Y. Bi, F. F. Cordero, H. B. Hartanto, M. Kraus, J. Nasufi, L. Reina and M. Worek, *On the modeling uncertainties of $t\bar{t}W^\pm$ multi-lepton signatures* (2021), [2109.15181](https://arxiv.org/abs/2109.15181).
- [28] A. Denner and G. Pelliccioli, *Combined NLO EW and QCD corrections to off-shell $t\bar{t}W$ production at the LHC*, Eur. Phys. J. C **81**(4), 354 (2021), doi:[10.1140/epjc/s10052-021-09143-3](https://doi.org/10.1140/epjc/s10052-021-09143-3), [2102.03246](https://arxiv.org/abs/2102.03246).
- [29] S. Actis, A. Denner, L. Hofer, A. Scharf and S. Uccirati, *Recursive generation of one-loop amplitudes in the Standard Model*, JHEP **04**, 037 (2013), doi:[10.1007/JHEP04\(2013\)037](https://doi.org/10.1007/JHEP04(2013)037), [1211.6316](https://arxiv.org/abs/1211.6316).
- [30] S. Actis, A. Denner, L. Hofer, J.-N. Lang, A. Scharf and S. Uccirati, *RECOLA: REcursive Computation of One-Loop Amplitudes*, Comput. Phys. Commun. **214**, 140 (2017), doi:[10.1016/j.cpc.2017.01.004](https://doi.org/10.1016/j.cpc.2017.01.004), [1605.01090](https://arxiv.org/abs/1605.01090).
- [31] A. Denner, S. Dittmaier and L. Hofer, *COLLIER: a fortran-based Complex One-Loop Library in Extended Regularizations*, Comput. Phys. Commun. **212**, 220 (2017), doi:[10.1016/j.cpc.2016.10.013](https://doi.org/10.1016/j.cpc.2016.10.013), [1604.06792](https://arxiv.org/abs/1604.06792).
- [32] A. Denner and M. Pellen, *NLO electroweak corrections to off-shell top-antitop production with leptonic decays at the LHC*, JHEP **08**, 155 (2016), doi:[10.1007/JHEP08\(2016\)155](https://doi.org/10.1007/JHEP08(2016)155), [1607.05571](https://arxiv.org/abs/1607.05571).
- [33] A. Denner, J.-N. Lang, M. Pellen and S. Uccirati, *Higgs production in association with off-shell top-antitop pairs at NLO EW and QCD at the LHC*, JHEP **02**, 053 (2017), doi:[10.1007/JHEP02\(2017\)053](https://doi.org/10.1007/JHEP02(2017)053), [1612.07138](https://arxiv.org/abs/1612.07138).
- [34] S. Catani and M. Seymour, *A general algorithm for calculating jet cross-sections in NLO QCD*, Nucl. Phys. B **485**, 291 (1997), doi:[10.1016/S0550-3213\(96\)00589-5](https://doi.org/10.1016/S0550-3213(96)00589-5), [Erratum: Nucl. Phys. B **510** (1998) 503–504], [hep-ph/9605323](https://arxiv.org/abs/hep-ph/9605323).
- [35] S. Dittmaier, *A general approach to photon radiation off fermions*, Nucl. Phys. B **565**, 69 (2000), doi:[10.1016/S0550-3213\(99\)00563-5](https://doi.org/10.1016/S0550-3213(99)00563-5), [hep-ph/9904440](https://arxiv.org/abs/hep-ph/9904440).
- [36] S. Catani, S. Dittmaier, M. H. Seymour and Z. Trócsányi, *The dipole formalism for next-to-leading order QCD calculations with massive partons*, Nucl. Phys. B **627**, 189 (2002), doi:[10.1016/S0550-3213\(02\)00098-6](https://doi.org/10.1016/S0550-3213(02)00098-6), [hep-ph/0201036](https://arxiv.org/abs/hep-ph/0201036).
- [37] A. Denner, S. Dittmaier, M. Roth and D. Wackerth, *Predictions for all processes $e^+e^- \rightarrow 4$ fermions + γ* , Nucl. Phys. **B560**, 33 (1999), doi:[10.1016/S0550-3213\(99\)00437-X](https://doi.org/10.1016/S0550-3213(99)00437-X), [hep-ph/9904472](https://arxiv.org/abs/hep-ph/9904472).
- [38] A. Denner, S. Dittmaier, M. Roth and D. Wackerth, *Electroweak radiative corrections to $e^+e^- \rightarrow WW \rightarrow 4$ fermions in double pole approximation: The RACOONWW approach*, Nucl. Phys. **B587**, 67 (2000), doi:[10.1016/S0550-3213\(00\)00511-3](https://doi.org/10.1016/S0550-3213(00)00511-3), [hep-ph/0006307](https://arxiv.org/abs/hep-ph/0006307).

- [39] A. Denner, S. Dittmaier, M. Roth and L. H. Wieders, *Electroweak corrections to charged-current $e^+e^- \rightarrow 4$ fermion processes: Technical details and further results*, Nucl. Phys. **B724**, 247 (2005), doi:[10.1016/j.nuclphysb.2011.09.001](https://doi.org/10.1016/j.nuclphysb.2011.09.001), [10.1016/j.nuclphysb.2005.06.033](https://doi.org/10.1016/j.nuclphysb.2005.06.033), [Erratum: Nucl. Phys. B **854** (2012) 504], [hep-ph/0505042](https://arxiv.org/abs/hep-ph/0505042).
- [40] A. Denner and S. Dittmaier, *The complex-mass scheme for perturbative calculations with unstable particles*, Nucl. Phys. B Proc. Suppl. **160**, 22 (2006), doi:[10.1016/j.nuclphysbps.2006.09.025](https://doi.org/10.1016/j.nuclphysbps.2006.09.025), [hep-ph/0605312](https://arxiv.org/abs/hep-ph/0605312).
- [41] A. Denner and S. Dittmaier, *Electroweak Radiative Corrections for Collider Physics*, Phys. Rept. **864**, 1 (2020), doi:[10.1016/j.physrep.2020.04.001](https://doi.org/10.1016/j.physrep.2020.04.001), [1912.06823](https://arxiv.org/abs/1912.06823).